

Mathematical Modeling of Metro Train-Induced Vibrations Using Finite Element Method



Naveen Kumar Kedia , Anil Kumar , and Yogendra Singh

Abstract Sustained economic and social growth in India has put a lot of pressure on existing urban traffic system. To overcome this problem several Indian cities has opted for the elevated and underground metro systems, for example New Delhi, Kolkata, Chennai and Jaipur metro. However, in the existing metro routes, due to movement of underground metro trains, vibration was felt at the nearby structures in the form of rattling of windows and door panels. Taking up the case study of Delhi metro, experimental data collected at the site showed that these vibrations have a frequency range of around 35–40 Hz when the traveling speed of the metro is around 40–50 kmph. Therefore, to address this issue a dynamic computational model for both the track and vehicle was developed with the use of finite element method. The whole system was divided into upper part consisting of vehicle body and the lower part consisting of slab track systems. The vehicle has been modeled as the lumped mass system, and slab track is modeled using finite element technique in which rail and slabs are modeled as two-noded beam element; the rail pads, fasteners and slab-resilient materials are represented by spring and damper elements. The interaction between the two parts was obtained through the forces developed between the wheel and the track, which is described by the nonlinear Hertzian contact theory. The primary cause of the force generation is the irregularity of the rail track profile which is modeled as the stationary ergodic Gaussian random process. The irregularity of the track profile is represented by the American Track Irregularity Power spectral

N. K. Kedia (✉)

Centre for Transportation Systems, Indian Institute of Technology Roorkee, Roorkee 247667, India

e-mail: naveen.kedia@outlook.com; nkedia@ct.iitr.ac.in

A. Kumar

Department of Mechanical and Industrial Engineering, Indian Institute of Technology Roorkee, Roorkee 247667, India

e-mail: anikrfme@iitr.ac.in

Y. Singh

Department of Earthquake Engineering, Indian Institute of Technology Roorkee, Roorkee 247667, India

e-mail: yogenfeq@iitr.ac.in

© Springer Nature Singapore Pte Ltd. 2021

E. J. Sapountzakis et al. (eds.), *Proceedings of the 14th International Conference on Vibration Problems*, Lecture Notes in Mechanical Engineering, https://doi.org/10.1007/978-981-15-8049-9_78

1209

density function of grade level 6 in the present study. The responses generated at the rail and slab are compared with the other models in the existing literature.

Keywords Wheel–rail interaction · Numerical methods · Coupled system · Slab track system

1 Introduction

The increase in urban population in India has led to the unbearable congestion and chaos to already degrading road traffic. To address the issue, underground trains have emerged as one of the most effective means to reduce road traffic as visible from other cities of the world. But transmission of vibration from metro trains to the structures lying nearby [1] experiences low-frequency vibration in the form of rattling of window panels and doors. To study this vibration propagation mechanism many modeling techniques are used by different authors in the past [2] which includes experimental data collection, numerical calculation using finite element method and theoretical method using classical equations of mechanics. Vibration propagation study can be done using either 2D or 3D models. Zhou et al. [3] used 2D theoretical model for simulating the steady response of a floating slab track–tunnel–soil system, Singh et al. [4] simulated the Delhi metro underground tunnel using PLAXIS 2D model, Hung et al. [5] considered 2D profile of the soil perpendicular to the railway track and used finite and infinite element for near- and far-field modeling and many other authors like [6–8] have used 2D model. The results obtained by the 2D models are approximate and qualitative in nature [9]. Since the train-track–tunnel–soil interaction system involves complex mechanism of vibration propagation, it becomes necessary to use 3D models as implemented by various authors like Auersch [10] who used 3D slab track models. Forest and Hunt [11] described an analytical 3D model for dynamics of the deep underground railway tunnel and Ma et al. [12] developed the 3D dynamic finite element model to study the impact of metro train-induced vibration on historic buildings.

In this paper the response of track system is studied under the influence of moving metro train inside the tunnel. A dynamic computational model similar to Lei and Noda [13] has been adopted for the vehicle and track coupling system. A vehicle is modeled as quarter-car in which primary and secondary suspension systems are considered and the track system is modeled using finite element model. It was studied by many authors like [14–18] that track profile irregularity is one of the major sources of vibration which further depends on train speed, axle load and volume of traffic. To study the wheel–rail dynamic forces, nonlinear Hertzian contact theory as used by Kacimi et al. [19] is adopted and random irregularity of the track profile is considered as Gaussian random process. The responses are generated at the rail and slab structure and the results are compared with the existing literature. Paper ends with the conclusions of the study.

2 Finite Element Formulation

A slab track considered in our study is similar to the CRTS II slab track which is a three-layer slab track system consisting of rail, precast slab and concrete support base as shown in Fig. 1. A discrete support of rail pads/fasteners lies between rail and precast slab, and a layer of cement mortar is provided between precast slab and concrete support layer/tunnel invert which have certain stiffness and damping properties. In the present study, a layer of hydraulically bonded layer (HBL) is considered between tunnel invert and tunnel lining and is represented as the continuous spring and damper elements. The hydraulic bonded layer is a family of cement bounded layer [20] and it consists of cement, lime, gypsum and coal fly ash, which set and harden in the presence of water. Below HBL, the model is considered rigid to confine the study area till the tunnel lining only.

The modeling of the track system is done using finite element in which rail, precast slab and concrete support layer is discretized as the 2D beam element having two nodes and each having two degrees of freedom. To cover the mid-frequency ranges of vibration, track length of 120 m is taken which is divided in the element size of 0.6 m, that is, distances between two continuous sleepers.

A typical beam element having two nodes and two degrees of freedoms can be represented as shown in Fig. 2.

Here v_i, v_j, θ_i and θ_j are the nodal displacements, and displacement at any point along the beam is expressed by the following expression:

$$v = N_1v_i + N_2\theta_i + N_3v_j + N_4\theta_j \tag{1}$$

where N_1-N_4 represent the displacement interpolation functions which are also a function of local coordinate x taken along the beam element. As per the sign

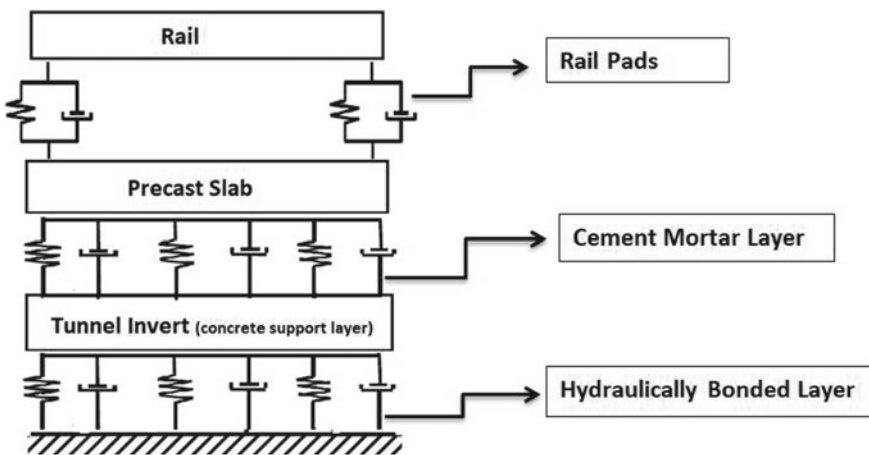
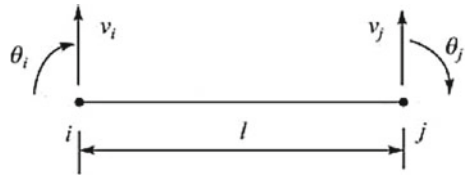


Fig. 1 Slab track element (not to scale)

Fig. 2 Beam element



convention shown in Fig. 2, the interpolation functions can be written as

$$N_1 = 1 - \frac{3x^2}{l^2} + \frac{2x^3}{l^3} \quad (2)$$

$$N_2 = -x + \frac{2x^2}{l} - \frac{x^3}{l^2} \quad (3)$$

$$N_3 = \frac{3x^2}{l^2} - \frac{2x^3}{l^3} \quad (4)$$

$$N_4 = \frac{x^2}{l} - \frac{x^3}{l^2} \quad (5)$$

Defining the element nodal displacement vector as

$$a = [v_i \ \theta_i \ v_j \ \theta_j]^T \quad (6)$$

Thus, Eq. 1 can be written as

$$f = Na \quad (7)$$

where

$$N = [N_1 \ N_2 \ N_3 \ N_4] \quad (8)$$

The mass matrix of the beam element is

$$[m]^e = \int_v \rho [N]^T [N] dv = \frac{\rho Al}{420} \begin{bmatrix} 156 & 22l & 54 & -13l \\ 22l & 4l^2 & 13l & -3l^2 \\ 54 & 13l & 156 & -22l \\ -13l & -3l^2 & -22l & 4l^2 \end{bmatrix} \quad (9)$$

The damping matrix of the beam element is

Similarly, mass matrix of the precast slab is

$$m_s = \frac{\rho_s A_s l}{420} \begin{bmatrix} 0 & 0 & 0 & 0 & 0 & 0 & 0 & 0 & 0 \\ 0 & 0 & 0 & 0 & 0 & 0 & 0 & 0 & 0 \\ 0 & 0 & 156 & -22l & 0 & 0 & 0 & 54 & 13l & 0 \\ 0 & 0 & -22l & 4l^2 & 0 & 0 & 0 & -13l & -3l^2 & 0 \\ 0 & 0 & 0 & 0 & 0 & 0 & 0 & 0 & 0 & 0 \\ 0 & 0 & 0 & 0 & 0 & 0 & 0 & 0 & 0 & 0 \\ 0 & 0 & 0 & 0 & 0 & 0 & 0 & 0 & 0 & 0 \\ 0 & 0 & 0 & 0 & 0 & 0 & 0 & 0 & 0 & 0 \\ 0 & 0 & 54 & -13l & 0 & 0 & 0 & 156 & 22l & 0 \\ 0 & 0 & 13l & -3l^2 & 0 & 0 & 0 & 22l & 4l^2 & 0 \\ 0 & 0 & 0 & 0 & 0 & 0 & 0 & 0 & 0 & 0 \\ 0 & 0 & 0 & 0 & 0 & 0 & 0 & 0 & 0 & 0 \end{bmatrix} \tag{15}$$

Mass matrix of the concrete support layer/tunnel invert is

$$m_t = \frac{\rho_t A_t l}{420} \begin{bmatrix} 0 & 0 & 0 & 0 & 0 & 0 & 0 & 0 & 0 \\ 0 & 0 & 0 & 0 & 0 & 0 & 0 & 0 & 0 \\ 0 & 0 & 0 & 0 & 0 & 0 & 0 & 0 & 0 \\ 0 & 0 & 0 & 0 & 0 & 0 & 0 & 0 & 0 \\ 0 & 0 & 0 & 156 & -22l & 0 & 0 & 54 & 13l \\ 0 & 0 & 0 & -22l & 4l^2 & 0 & 0 & -13l & -3l^2 \\ 0 & 0 & 0 & 0 & 0 & 0 & 0 & 0 & 0 \\ 0 & 0 & 0 & 0 & 0 & 0 & 0 & 0 & 0 \\ 0 & 0 & 0 & 0 & 0 & 0 & 0 & 0 & 0 \\ 0 & 0 & 0 & 0 & 0 & 0 & 0 & 0 & 0 \\ 0 & 0 & 0 & 0 & 0 & 0 & 0 & 0 & 0 \\ 0 & 0 & 0 & 54 & -13l & 0 & 0 & 156 & 22l \\ 0 & 0 & 0 & 13l & -3l^2 & 0 & 0 & 22l & 4l^2 \end{bmatrix} \tag{16}$$

Mass matrix of the whole element can be written as

$$m = m_r + m_s + m_t \tag{17}$$

Using the similar concept of matrix formulation, stiffness matrix for the whole element can be written as

$$k = k_r + k_s + k_t + k_p + k_c + k_h \tag{18}$$

Here, k_r, k_s, k_t, k_p, k_c and k_h are the stiffnesses of rail beam, precast slab, tunnel invert, rail pads, cement mortar layer and HBL layer, respectively.

Damping matrix for the whole element can be written as

$$c = c_r + c_p + c_c + c_h \tag{19}$$

Here, c_r represents the proportional damping matrix of the rail, precast slab and tunnel invert. It is represented as

$$c_r = \alpha m_r + \beta k_r + \alpha m_s + \beta k_s + \alpha m_t + \beta k_t \tag{20}$$

The Rayleigh damping coefficients α and β depend on the damping ratio and the natural frequencies of the system. c_p , c_c and c_h are damping of rail pads, cement mortar layer and HBL layer, respectively.

Now, using the general rule of assembling element matrix, the global mass, stiffness, damping and load matrix are assembled and the final dynamic equation of the whole system is written as

$$M_{N \times N} \ddot{a}(t)_{N \times 1} + C_{N \times N} \dot{a}(t)_{N \times 1} + K_{N \times N} a(t)_{N \times 1} = Q(t)_{N \times 1} \tag{21}$$

Here, N is the degree of freedom of system.

3 Vehicle Model

A simplified model of the train represented as quarter-car is taken in the present study to understand the interaction between a wheel and a rail. The model consists of primary and secondary suspension spring and damper system as shown in Fig. 3 moving with constant velocity over a rail.

Using law of mechanics, the equations of motion of the above system which is a second-order differential equation can be written in the matrix form as follows

$$M_v \ddot{a}_v + C_v \dot{a}_v + K_v a_v = Q_v \tag{22}$$

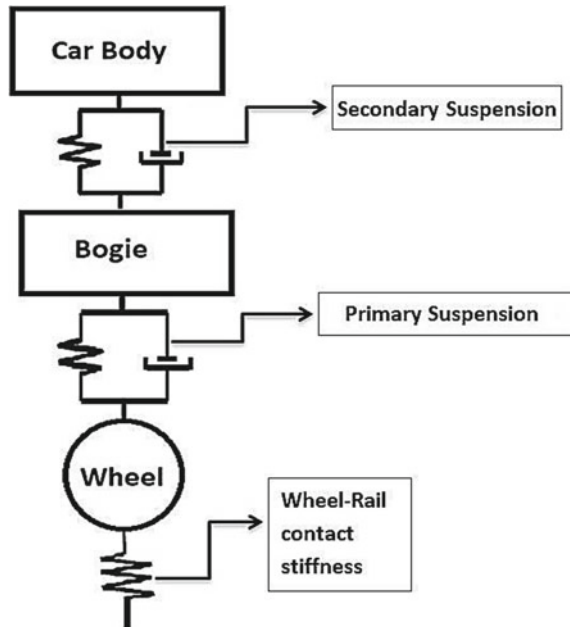
Here,

$$M_v = \text{diag}[m_{cr} \ m_{bo} \ m_{wh}] \tag{23}$$

$$C_v = \begin{bmatrix} c_{cr} & -c_{cr} & 0 \\ -c_{cr} & c_{cr} + c_{bo} & -c_{bo} \\ 0 & -c_{bo} & c_{bo} \end{bmatrix} \tag{24}$$

$$K_v = \begin{bmatrix} k_{cr} & -k_{cr} & 0 \\ -k_{cr} & k_{cr} + k_{bo} & -k_{bo} \\ 0 & -k_{bo} & k_{bo} \end{bmatrix} \tag{25}$$

Fig. 3 Quarter-car model



$$Q_v = \begin{bmatrix} -m_{cr}g \\ -m_{bog}g \\ -m_{wh}g + P \end{bmatrix} \tag{26}$$

'P' is the wheel-rail interaction force arising due to a relative displacement between wheel and rail at the contact point.

4 Wheel-Rail Interaction

The interaction between the two subsystems, that is, vehicle and track is achieved through the wheel-rail interaction forces arising at the rail-wheel interface. Many theories have been put forward to study the interaction forces. In the present study nonlinear Hertzian contact theory had been used to generate the contact forces.

$$P = \begin{cases} \frac{1}{G^{1.5}} |v_{wi} - (v_{ri} + \eta_i)|^{1.5} & \text{if } |v_{wi} - (v_{ri} + \eta_i)|^{1.5} < 0 \\ 0 & \text{if } |v_{wi} - (v_{ri} + \eta_i)|^{1.5} > 0 \end{cases} \tag{27}$$

Equation (27) represents the contact forces in which v_{wi} , v_{ri} and η_i are wheel displacement, rail displacement and irregularity, respectively, at the i th wheel rail contact point and is a function of speed of a train. As discussed by authors like [21, 22] in their study that for ground vibrations study vertical track irregularities are

predominant factor for vibration generation, thus vertical random track irregularities are considered in this paper, which is generated based on the power spectrum density(PSD) formula given by the Federal Railroad Administration of America (FRA). For the metro vibrations generally grade 5 or grade 6 track PSD function is used to generate the random track irregularity.

4.1 Solution Method

The dynamic responses of the rail and track system are solved separately using the Newmark integration scheme in which if solution at time step ‘ t ’ is known then the solution at time step ‘ $t + dt$ ’ can be obtained by using the following formula

$$(K + a_1M + a_2C)a^{t+dt} = Q^{t+dt} + M(a_1a^t + a_3\dot{a}^t + a_4\ddot{a}^t) + C(a_2a^t + a_5\dot{a}^t + a_6\ddot{a}^t) \quad (28)$$

Here, a_1 to a_6 are the Newmark constants.

Since the Hertzian forces acting at the wheel–rail contact point is nonlinear in nature, thus it becomes important to iterate the value at each time using suitable iteration technique as suggested by Yang and Fonder [23] at each time step of Newmark till the required convergence criteria is fulfilled.

5 Results and Discussions

The vehicle and track parameters used in this study are of CRH3 train and CRTS II slab track, respectively. The following assumptions are made:

- In the present analysis only bouncing vibration of the vehicle is considered.
- Due to symmetry of the system only half of the vehicle track coupling system is used for the analysis.
- At initial time step it is assumed that wheel–rail interaction force is solely due to the irregularity of the track.
- The relative displacement between wheel and track is assumed to be zeros at initial time step.
- The convergence range considered in the iteration technique lies between 10^{-5} and 10^{-10} .

The purpose of this study is to validate our model with existing available literature so that a full-scale model can be developed for our case study of Delhi Metro. To validate our data, responses generated in the proposed model are compared with the results of Lei et al. [24], for same track length and vehicle speed.

The comparison done in Table 1 clearly indicates that the order of result obtained in both the models is the same. Though the results don't match exactly which might be due to the differences in the track properties and the vehicle model taken, we can say that the proposed model can be used to study the vibration generation due to the metro trains and to get a more realistic data a full-scale model of the vehicle, and a track system can be developed based on the methodology discussed in this paper.

Then, to study the behavior of the responses generated by the model, a track length of 120 m is taken and vehicle is made to run at two different speeds of 10 and 40 m/s. Track irregularity as shown in Fig. 4 is used in this study.

- For $L = 120$ and $v = 10$ m/s
- For $L = 120$ m and $v = 40$ m/s

Figures 5 and 8 show that amplitude of the wheel-rail interaction force increases with the increase in speed of the vehicle. Moreover, the midpoint deflection of the rail also increases with the increase in speed as visible from Figs. 6 and 9. A similar

Table 1 Comparison of results

S. no.	Parameters	Present study		Lei et al. [24]	
		Max.	Min.	Max.	Min.
1	Rail displacement	0.16 mm	-2.01 mm	0.16 mm	-1.30 mm
2	Rail acceleration	535 m/s ²	-680 m/s ²	206.82 m/s ²	-203.03 m/s ²
3	Wheel acceleration	93.5 m/s ²	-64.3 m/s ²	46.64 m/s ²	-40.40 m/s ²

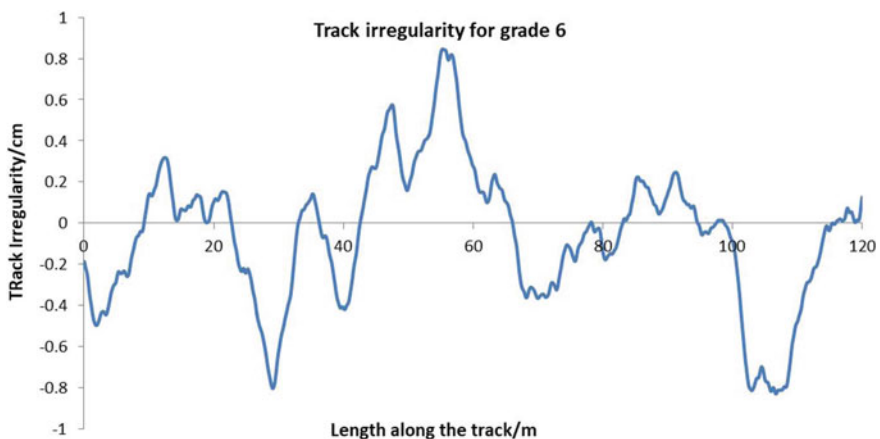


Fig. 4 Track irregularity

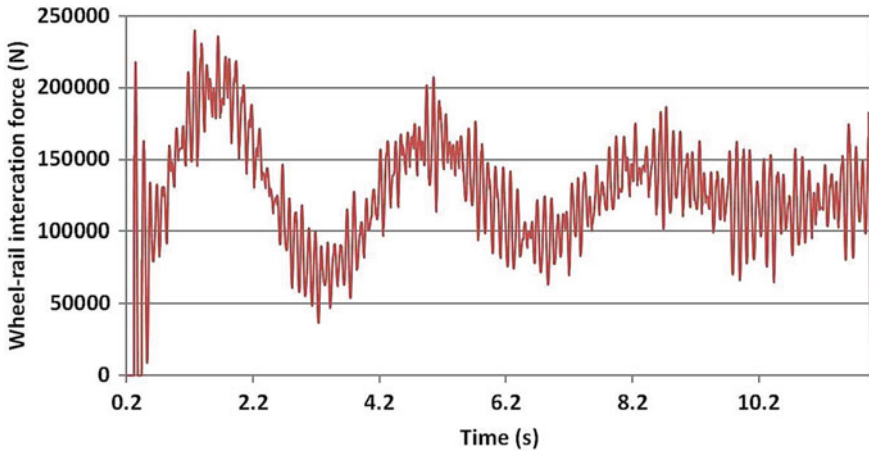


Fig. 5 Wheel-rail interaction force

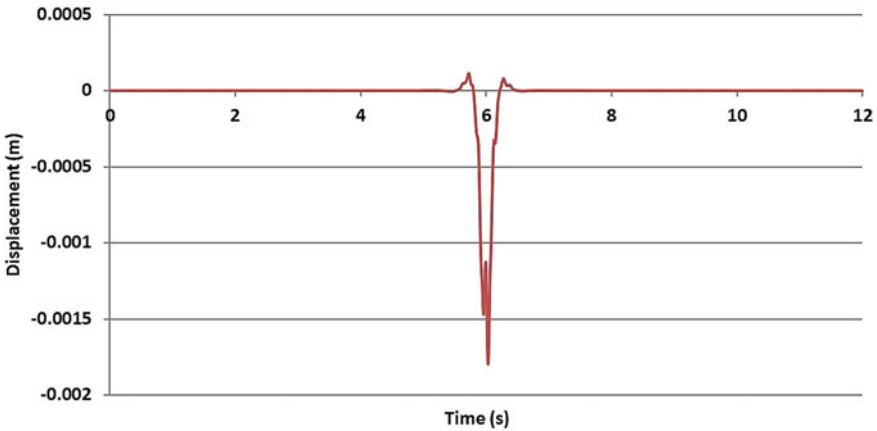


Fig. 6 Midpoint deflection of rail

trend was observed for the acceleration computed at the midpoint of the rail, which can be seen in Figs. 7 and 10.

6 Conclusions

The responses generated from the coupled model of vehicle and slab track were compared with those existing in the literature. Since the results obtained were of the same order we can conclude that the model adopted in the present paper can be used to study the dynamic responses of train-track-tunnel-soil system generated through the wheel-rail interaction. To capture a more realistic behavior a full-scale model of

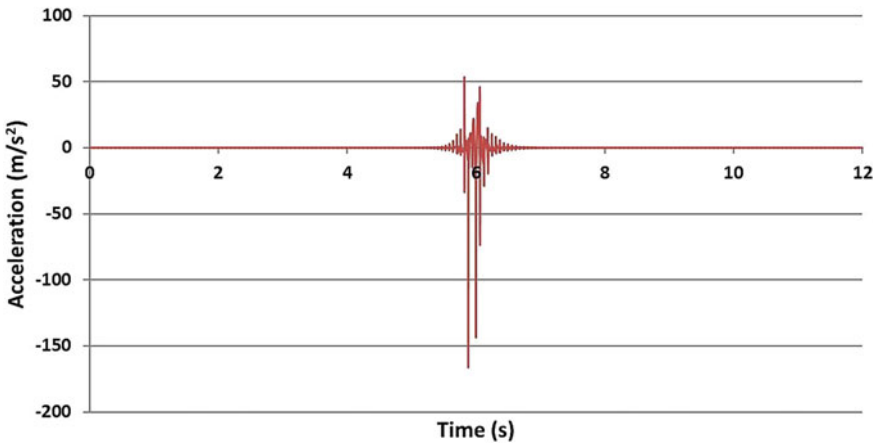


Fig. 7 Midpoint acceleration of rail

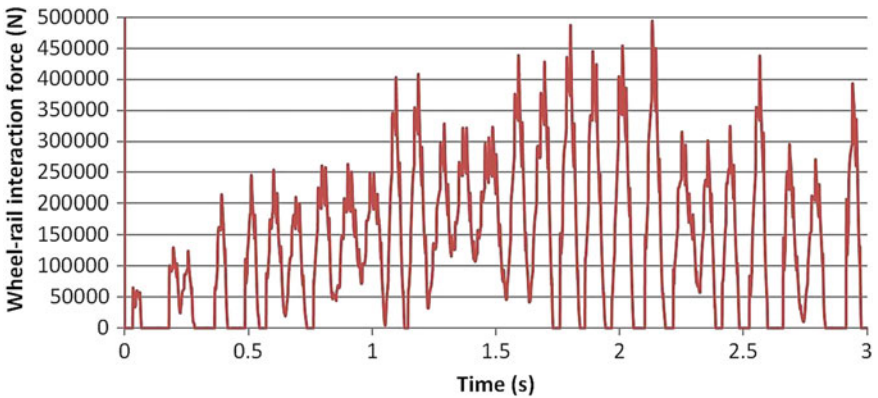


Fig. 8 Wheel-rail interaction force

vehicle and slab track considering more degrees of freedom can be developed based on the computation technique discussed in this paper.

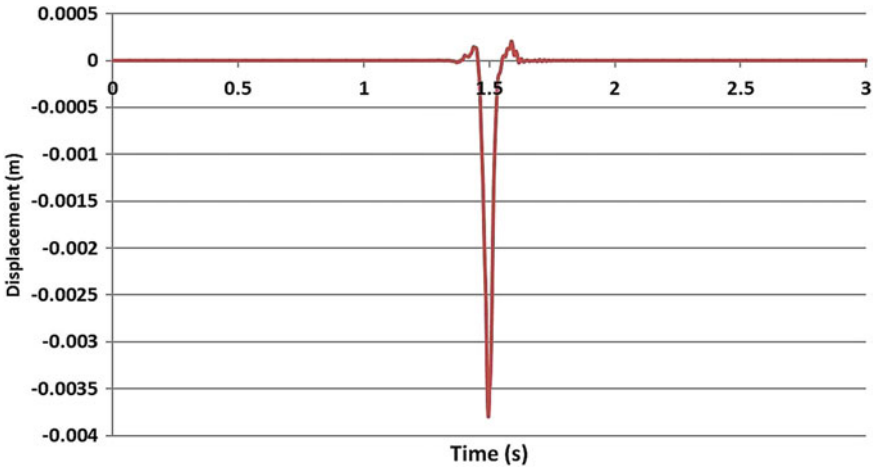


Fig. 9 Midpoint deflection of rail

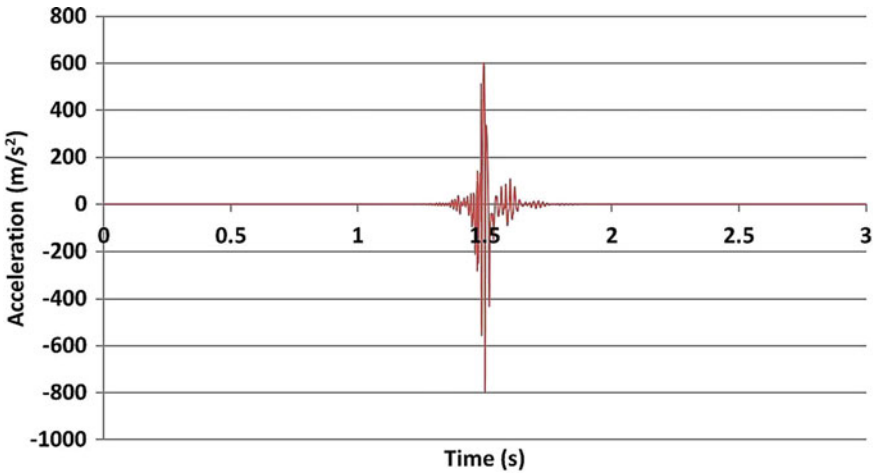


Fig. 10 Midpoint acceleration of rail

References

1. Forrest JA, Hunt HEM (2006) A three-dimensional tunnel model for calculation of train-induced ground vibration. *J Sound Vib* 294(4-5):678-705. <https://doi.org/10.1016/j.jsv.2005.12.032>
2. Liu Z, Cui G, Wang X (2014) Vibration characteristics of a tunnel structure based on soil-structure interaction. *Int J Geomech* 14(4):1-8. [https://doi.org/10.1061/\(ASCE\)GM.1943-5622.0000357](https://doi.org/10.1061/(ASCE)GM.1943-5622.0000357)

3. Zhou B, Xie X-Y, Yang YB (2014) Simulation of wave propagation of floating slab track-tunnel-soil system by 2D theoretical model. *Int J Struct Stab Dyn* 14(01):1–24. <https://doi.org/10.1142/S021945541350051X>
4. Singh M, Viladkar MN, Samadhiya NK (2017) Seismic analysis of Delhi metro underground tunnels. *Indian Geotech J* 47(1):67–83. <https://doi.org/10.1007/s40098-016-0203-9>
5. Hung HH, Chen GH, Yang YB (2013) Effect of railway roughness on soil vibrations due to moving trains by 2.5D finite/infinite element approach. *Eng Struct* 57:254–266. <https://doi.org/10.1016/j.engstruct.2013.09.031>
6. Chua KH, Balendra T, Lo KW (1992) Groundborne vibrations due to trains in tunnels. *Earthq Eng Struct Dyn* 21(5):445–460. <https://doi.org/10.1002/eqe.4290210505>
7. Alves Costa P, Calçada R, Silva Cardoso A (2012) Ballast mats for the reduction of railway traffic vibrations. Numerical study. *Soil Dyn Earthq Eng* 42:137–150. doi: <https://doi.org/10.1016/j.soildyn.2012.06.014>
8. Xu Q, Xiao Z, Liu T, Lou P, Song X (2015) Comparison of 2D and 3D prediction models for environmental vibration induced by underground railway with two types of tracks. *Comput Geotech* 68:169–183. <https://doi.org/10.1016/j.compgeo.2015.04.011>
9. Yang YB, Hung HH (2008) Soil vibrations caused by underground moving trains. *J Geotech Geoenviron Eng* 134(11):1633–1644. [https://doi.org/10.1061/\(ASCE\)1090-0241\(2008\)134:11\(1633\)](https://doi.org/10.1061/(ASCE)1090-0241(2008)134:11(1633))
10. Auersch L (2012) Dynamic behavior of slab tracks on homogeneous and layered soils and the reduction of ground vibration by floating slab tracks. *J Eng Mech* 138(8):923–933. [https://doi.org/10.1061/\(ASCE\)EM.1943-7889.0000407](https://doi.org/10.1061/(ASCE)EM.1943-7889.0000407)
11. Forrest JA, Hunt HEM (2006) Ground vibration generated by trains in underground tunnels. *J Sound Vib* 294(4–5):706–736. <https://doi.org/10.1016/j.jsv.2005.12.031>
12. Ma M, Liu W, Qian C, Deng G, Li Y (2016) Study of the train-induced vibration impact on a historic Bell Tower above two spatially overlapping metro lines. *Soil Dyn Earthq Eng* 81:58–74. <https://doi.org/10.1016/j.soildyn.2015.11.007>
13. Lei X, Noda N-A (2002) analyses of dynamic response of vehicle and track coupling system with random irregularity of track vertical profile. *J Sound Vib* 258(1):147–165. <https://doi.org/10.1006/jsvi.2002.5107>
14. Bai L, Liu R, Sun Q, Wang F, Xu P (2015) Markov-based model for the prediction of railway track irregularities. *Proc Inst Mech Eng Part F J Rail Rapid Transit* 229(2):150–159. doi: <https://doi.org/10.1177/0954409713503460>
15. Haigermoser A, Lubber B, Rauh J, Gräfe G (2015) Road and track irregularities: measurement, assessment and simulation. *Veh Syst Dyn* 53(7):878–957
16. Nokhbatolfighahai A, Noorian MA, Haddadpour H (2018) Dynamic response of tank trains to random track irregularities. *Meccanica* 53(10):2687–2703. <https://doi.org/10.1007/s11012-018-0849-8>
17. Ananthanarayana N (1988) Track irregularity limits from consideration of track-vehicle interaction. *Math Comput Model* 11:932–935. doi:[https://doi.org/10.1016/0895-7177\(88\)90630-9](https://doi.org/10.1016/0895-7177(88)90630-9)
18. Perrin G et al (2013) Track irregularities stochastic modeling. *Prob Eng Mech* 34:123–130. <https://doi.org/10.1016/j.probenmech.2013.08.006>
19. El Kacimi A, Woodward PK, Laghrouche O, Medero G (2013) Time domain 3D finite element modelling of train-induced vibration at high speed. *Comput Struct* 118:66–73. <https://doi.org/10.1016/j.compstruc.2012.07.011>
20. Nandhini M, Jaghan S (2016) Design of hydraulic bound layer for ballastless track. *J Chem Pharm Sci* 9(4):2316–2319
21. Mu D, Choi DH (2014) Dynamic responses of a continuous beam railway bridge under moving high speed train with random track irregularity. *Int J Steel Struct* 14(4):797–810. <https://doi.org/10.1007/s13296-014-1211-1>
22. Podwórna M (2015) Modelling of random vertical irregularities of railway tracks. *Int J Appl Mech* 20(3):647–655. <https://doi.org/10.1515/ijame-2015-0043>

23. Yang F, Fonder GA (1995) An iterative solution method for dynamic response of bridge-vehicles systems. *Earthq Eng Struct Dyn* 25:195–215
24. Lei X, Wu S, Zhang B (2016) Dynamic analysis of the high speed train and slab track nonlinear coupling system with the cross iteration algorithm. *J Nonlinear Dyn* 2016(8356160):1–17. <https://doi.org/10.1155/2016/8356160>